

3D COUPLED MECHANICAL AND HYDRAULIC MODELING OF THE COLUMN-SUPPORTED EMBANKMENT IN HIGHWAY WIDENING PROJECT

J. H. Song¹ and L. C. Miao²

ABSTRACT: Numerical studies were conducted to improve the understanding of the behavior of column-supported embankments in highway widening project. Due to the complexity of the problem, so far, consolidation process and three-dimensional patterns of columns have not been well simulated in most published numerical studies. As a result, the time-dependant behavior and the serviceability of this system have not been well evaluated. In this study, a three-dimensional coupled mechanical and hydraulic modeling was conducted using ABAQUS to consider consolidation and three-dimensional arrangement of columns. The numerical predictions are analyzed in terms of settlements and increments in vertical effective stresses. Firstly, the effectiveness of the use of columns and caps is studied. Afterwards, a parametric analysis is performed to study the influence on the soil-columns and caps system of the deformability and the effective friction angle of the embankment. At last some conclusions are obtained from the result of the numerical calculation.

Keywords: Highway widening project, embankment on soft clay, column-supported embankments, columns and caps, numerical analysis.

INTRODUCTION

It is necessary to increase highway capacities by widening embankments and pavements because of the increased traffic volume after construction. The new embankment can cause additional deformations under the widened portion and the existing embankment. Differential settlement can develop between the new and existing embankment. Excessive differential settlements can cause pavement cracking (Han et al. 2006).

Now widening of embankment has been commonly adopted in China such as the widening projects in Yangzhou China illustrated in Fig. 1. But up to now very few guidance for design is available for widening projects (Han et al. 2007). Numerical studies have been more often adopted due to their cost and time efficiency and flexibility as compared with experimental studies. Han (2007) carried out the analyses of eight cases of column-supported widened embankments. Some recommendations for the design of foundation columns to remedy roadway pavement failure due to widening of embankments were given. So far, it is not well understood how foundation columns should be designed and laid out to reach desired performance.

The FEM analysis has greatly improved our knowledge on the columns supported embankments.

However, due to the complexity of the problem, two important aspects of the problem have not been well investigated (Huang et al. 2009a). Firstly, in lieu of three-dimensional modeling, two-dimensional simulation was used in most of the numerical studies (Porooshab et al. 1997; Huang et al. 2009b; Abusharar SW et al. 2011), which is sufficient when columns under embankments are installed in a wall pattern along the traffic direction but not sufficient when columns are installed isolated from each other (Zheng et al. 2008). Secondly, consolidation was excluded in most numerical modeling of this problem. However, the columns supported embankments are often constructed over soft soils with a high ground water table and consolidation occurs during and after construction (Terzaghi 1943). In other words, the columns supported embankments over soft soils have time dependant behavior. To avoid the complexity of numerical analyses, most researchers have chosen to analyze the long-term or short term behavior of the columns supported embankments by assigning drained or undrained parameters correspondingly (Forsman and Uotinen 1999; Wang and Huang 2004). Under these two conditions, the behavior of the columns supported embankments is not framed in a time domain. Therefore, post construction performance of the columns supported embankments, which is important to

¹ School of Civil Engineering and Architecture, Henan University of Technology, 100 Lianhua Street, Zhengzhou 450001, CHINA

² Institute of Geotechnical Engineering, Southeast University, 35 Jinxianghe Road, Xuanwu District, Nanjing 221008, CHINA

Note: Discussion on this paper is open until June 2014

evaluate their serviceability, cannot be studied (Han et al. 2006).



Fig. 1 The pavement widening projects in Yangzhou China.

In practice, a post-construction settlement is more critical and meaningful to the serviceability of the structures on the embankment. Therefore, an accurate calculation of post-construction settlements at different service life periods requires a coupled mechanical and hydraulic analysis. ABAQUS is a proper software to solve the coupled mechanical and hydraulic problem. Some of the common coupled pore fluid diffusion/stress analysis problems that can be analyzed with ABAQUS are: saturated flow, partially saturated flow, combined heat transfer and pore fluid flow. Saturated flow is that the soil mechanics problems generally involve fully saturated flow, since the solid is fully saturated with ground water. Typical examples of saturated flow include consolidation of soils under foundations and excavation of tunnels in saturated soil.

The objective of this study is to investigate the effects of installing foundation columns with/without caps in the soil beneath the widened portion of the embankment including the deformation and the stress evolution with time due to the dissipation of pore pressure. The study was carried out using ABAQUS as a three dimensional FE software. This work is divided into two parts. The first part corresponds to the analysis of an embankment of infinite dimensions built on soft soil reinforced with columns and caps. The results are discussed in terms of settlements and increments in vertical effective stresses. In the second part, a parametric analysis is performed to study the influence on the soil-columns and caps system of the deformability and the effective friction angle of the embankment.

NUMERICAL MODELLING OF THE HIGHWAY WIDENING PROJECT

The real highway widening project in Yangzhou China is illustrated in Fig. 2. Due to the symmetry of the

cross-section and the repetition of the span along the traffic direction, half of the cross-section and half span along the traffic direction were simulated to save computing time (Abusharar 2009). The cross-section, boundary conditions, and dimensions for the numerical model used for this study are presented in Fig. 3. Fig. 4 shows the FE mesh used in the analysis consisting of 28398 eight-noded isoparametric octahedral elements and 30747 nodal points.

Table 1 shows the soil properties used in the numerical analysis. Table 2 shows the embankment and column properties used in the numerical analysis. Embankment fill, soft soil, and columns are modeled as linearly elastic perfectly plastic materials with Mohr–Coulomb failure criteria.

Table 1 Soil properties used in the numerical analysis

Soil Layer	Thickness (m)	γ (kN/m ³)	Void ratio	E (MPa)	c (kPa)	ϕ' (°)	K (m/s)
①	1.75	19.5	0.736	7.7	19	20	1×10^{-7}
②	5.75	18.9	0.866	12.4	10	24.1	8.51×10^{-8}
③	8.5	19.3	0.755	19.0	9	28.8	1.19×10^{-9}
④	12	19.3	0.750	24.2	8	28.9	3.57×10^{-9}
⑤	9.15	18.6	0.862	24.3	9	26.1	8.32×10^{-9}
⑥	7.6	18.1	0.950	17.3	12	22.2	5.73×10^{-9}
⑦	5.25	18.9	0.754	34.8	6	31.2	5.73×10^{-9}

Note: E: elastic modulus; c: unit weight; c' : effective cohesion; ϕ' : effective friction angle; K: permeability coefficient; γ : unit weight.

Table 2 Embankment and column properties used in the numerical analysis

Material	γ (kN/m ³)	Void ratio	E (MPa)	c (kPa)	ϕ' (°)
Embankment	19	0.6	15	10	35
column	20	/	2000	/	/

Note: Damage of the column is not considered in this analysis.

The mechanical boundary conditions were such that both lateral vertical sides were restrained from moving in the horizontal direction, while the bottom boundary was restrained from moving in both directions (Fig. 3). In the cross-section view, the left boundary was assumed impervious considering no flow crossing the symmetry plane. The right boundary was assumed impervious because it was located far enough to have minor influence on the results. The bottom was also assumed impervious to account for the low permeability of the layer below. In the plane view, the two sides perpendicular to the traffic direction were assumed impervious due to the symmetry and the repetition of the half span.

In order to simulate the consolidation phenomenon, elements with eight nodal degrees of freedom were used below the water table, providing quadratic interpolation of displacements and linear interpolation of pore pressures and thereby allowing the calculation of the displacements in eight nodes and the excess pore pressure in four corner nodes.

All the columns started from the base of the embankment and were embedded into the deep soil, as illustrated in Fig. 3.

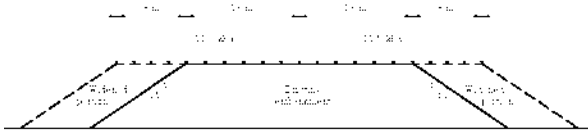


Fig. 2 The real embankment of roadway widening

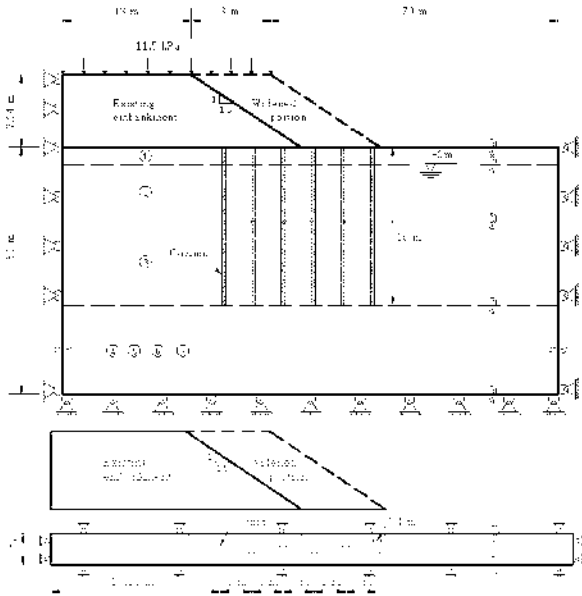


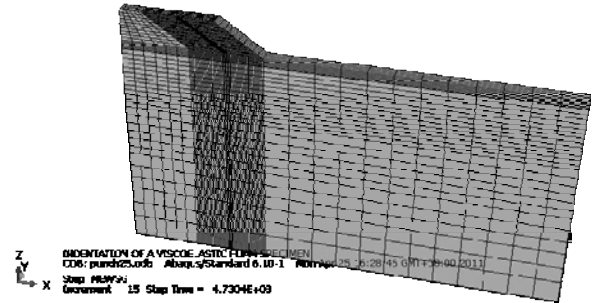
Fig. 3 Model for the numerical analysis of roadway widening

The columns in the real project are pipe piles and they are made of steel reinforced concrete. In the numerical model the contact area between the column and soil is supposed to be glued to each other. Such the numerical model can be established easier.

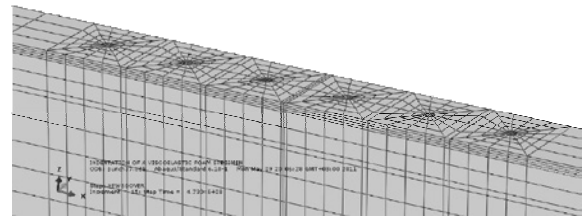
In the research by Huang et al. (2009), the circular isolated columns were approximated by square columns of equivalent area to simplify the numerical modeling using FLAC3D, as illustrated in Fig. 5. This method is not calibrated by contrast to the result of circular columns. In this study, the model of column is built as circular columns as illustrated in Fig. 4.

In the numerical calculation, the ground was first formed by applying a gravity force. Then the existing

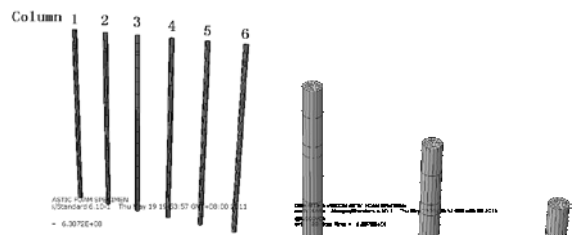
embankment was constructed and followed by a traffic loading of 11.5 kPa. After ten years of consolidation, the widened portion and the traffic loading on the widened portion were added. The construction of the embankment consists of four sub-layers, each one with a 1.84 m thickness applied at a time delay of 10 days.



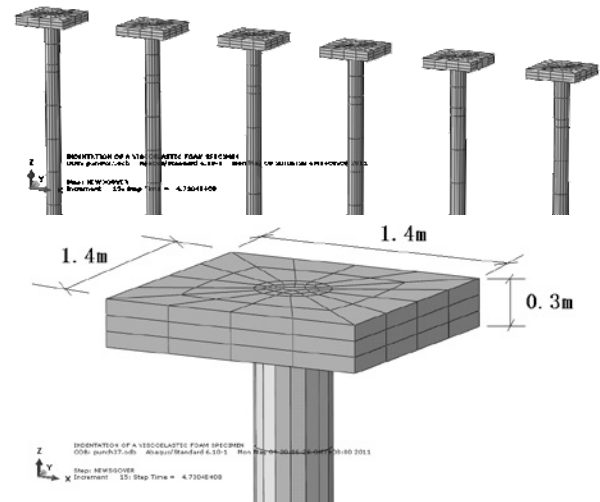
(a) Whole model



(b) Model below the embankment



(c) Columns



(d) Columns and caps

Fig. 4 FE mesh of the numerical model

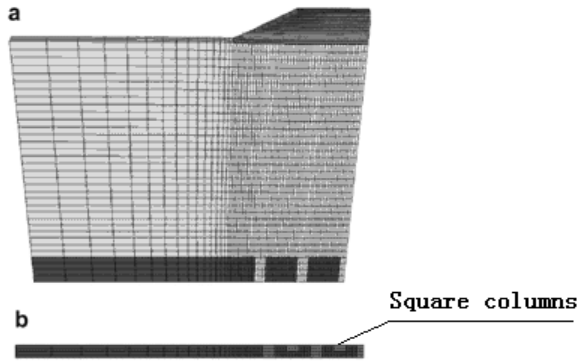


Fig. 5 FLAC3D model build by Jie Huang: (a) Elevation view; (b) plan view (Huang and Han 2009).

ANALYSIS OF THE RESULTS

Settlement

The settlement at the base of the embankment over time with different conditions is illustrated in Fig. 6. The results show that the inclusion of columns causes the decrease of the maximum settlement. At the same time, the column reinforcement induces differential settlements between the soil and the column. And it also can be concluded that the differential settlements is reduced when the caps are used.

Fig. 6 shows that the minimum settlement is at $x=0$. And the minimum settlement can be reduced when the columns is used. But the minimum settlement can not be reduced when the caps is used.

Fig. 6 also shows differential settlements between column and soil, which naturally is caused by the greater deformability of the soil compared to column. These differential settlements increase slightly over time. The differential settlements of the different column are different. The differential settlements of column 3 and column 4 are larger than column 1 and column 6.

The settlements at the crest of the embankment with different conditions are illustrated in Fig. 7. The results show that the inclusion of columns causes the decrease of the maximum settlement. But the inclusion of caps can not decrease the maximum settlement. This is because the elastic modulus and effective friction angle of the embankment are significantly large.

The transversal evolution of the vertical displacement shows no pattern with depth (Fig. 8), whereas close to the surface there is a region ($z > -10.7m$) in which the vertical displacement in the soil is higher than in the columns. In the deep region ($z < -10.7m$) the vertical displacement in the columns is higher than in the soil. The result has a good agreement to Venda Oliveira PJ (2011).

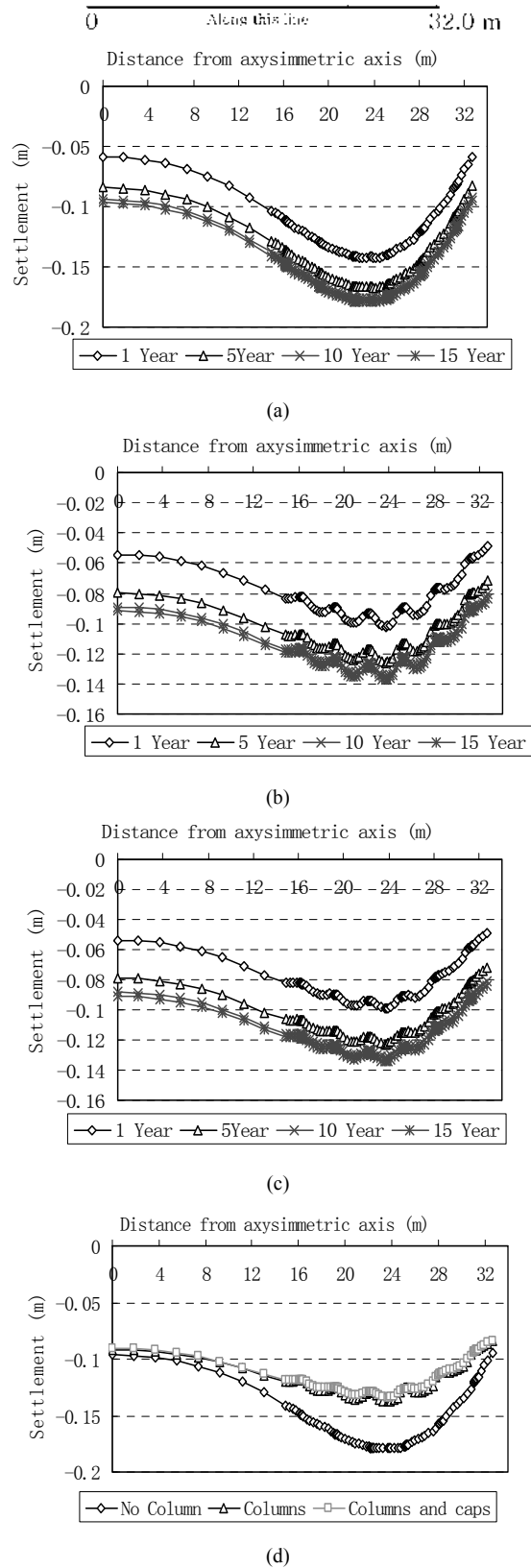


Fig. 6 Settlements at the base of the embankment: (a) No column; (b) Columns; (c) Columns and caps and (d) Contrast of the different conditions

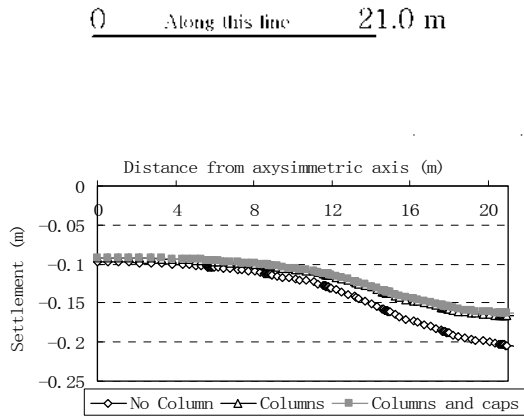


Fig. 7 Settlements at the crest of the embankment

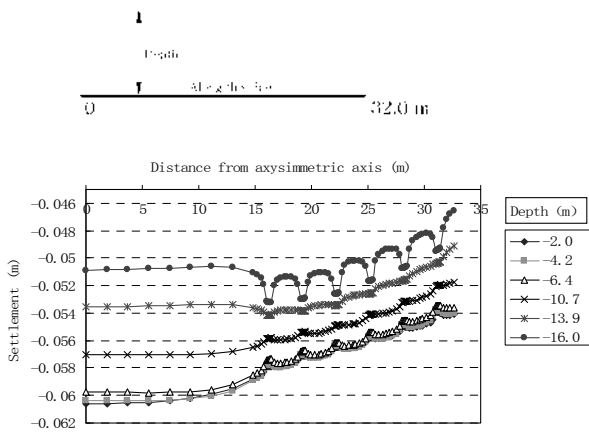


Fig. 8 Settlements for different depths

Vertical stress at the base of the embankment

Fig. 9 shows the vertical stress contours of the soil. The diagrams in Fig. 10 show the evolution of the increments of vertical effective stresses along the transversal section ($z = 0$). The diagrams in Fig. 11 show the vertical effective stresses along the transversal section ($z = 0$) with different conditions.

As illustrated in Fig. 9, the columns change the stress distribution in the soil. The stress concentration is appeared at bottom and top of the column. When the caps are used, the stress concentration is attenuated at the top of the column.

As illustrated in Fig. 10, with the development of consolidation the vertical effective stresses in the columns increases and the columns is subjected to absorbing nearly the entire load applied by the embankment. The figures also show that the vertical effective stresses in the soil is negligible compared to the columns, in which the increments are quite high as a result of the arching effect.

As illustrated in Fig. 11, when the caps are used, the concentrated stress near the columns is reduced. This is because the bearing area of the caps is larger than the columns only.

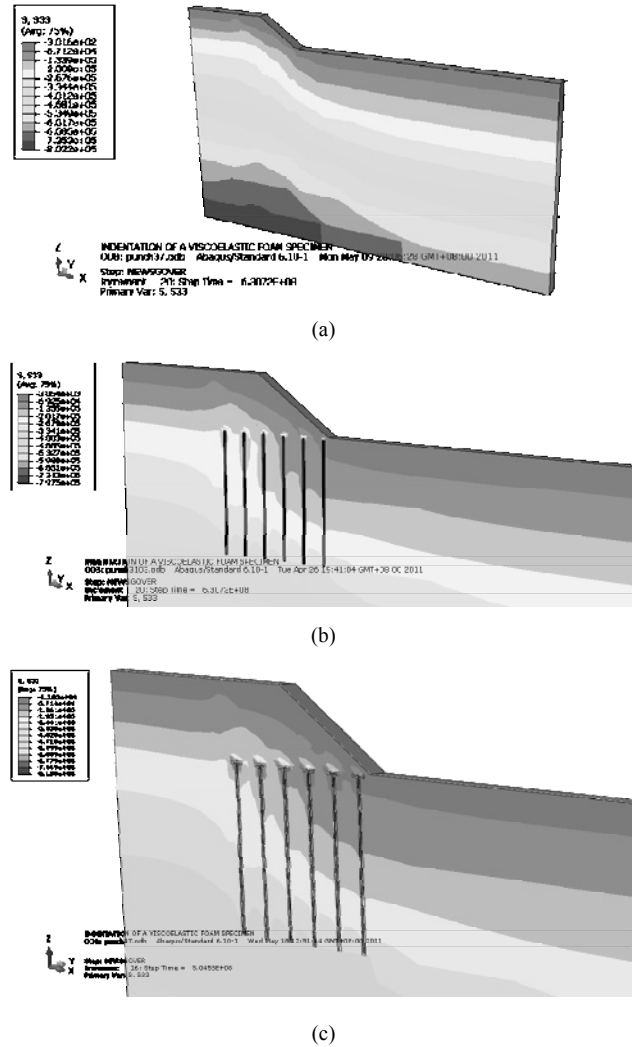


Fig. 9 Vertical stress contours of the soil: (a) With no columns; (b) With columns and (c) With columns and caps

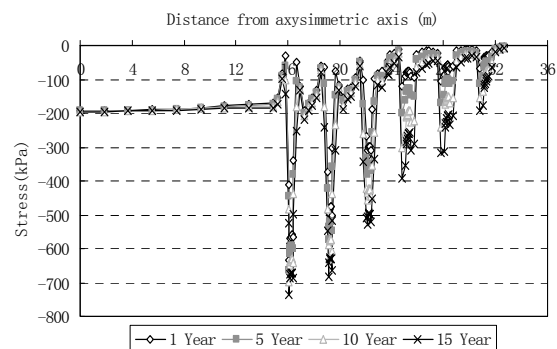


Fig. 10 Evolution of the increments of vertical effective stresses at the base of the embankment

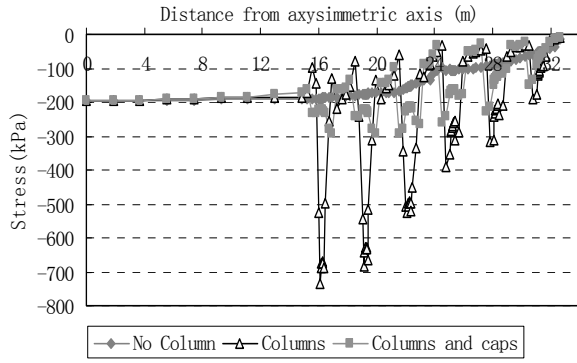


Fig. 11 Vertical effective stresses at the base of the embankment with different conditions

Vertical stresses in the columns and soil

The diagrams in Fig. 12 show the vertical effective stresses in the different columns at T = 15 year. The diagrams in Fig. 13 and Fig. 14 show the evolution of the increments of vertical effective stresses in the column and soil with depth respectively.

Fig. 12 shows that the vertical effective stresses in the different columns are different. The vertical effective stresses in column 4 are the largest and the vertical effective stresses in column 1 and column 6 are smallest. Fig. 13 shows that the vertical effective stresses in the columns increases with time. Fig. 14 shows that the soil effective stress increments near the bottom of the columns are lager. Fig. 15 shows the evolution of excess pore pressures in the soil with depth. The excess pore water pressure decreases with time and the soil effective stress increases as a result.

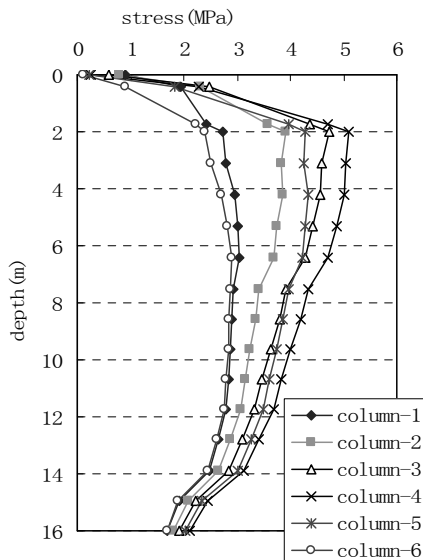


Fig. 12 Vertical effective stresses in the different columns at T=15year

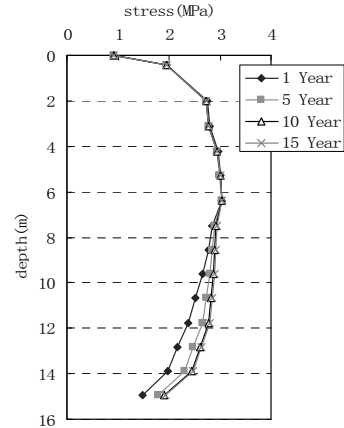


Fig. 13 Increments of vertical effective stress with depth in column 1

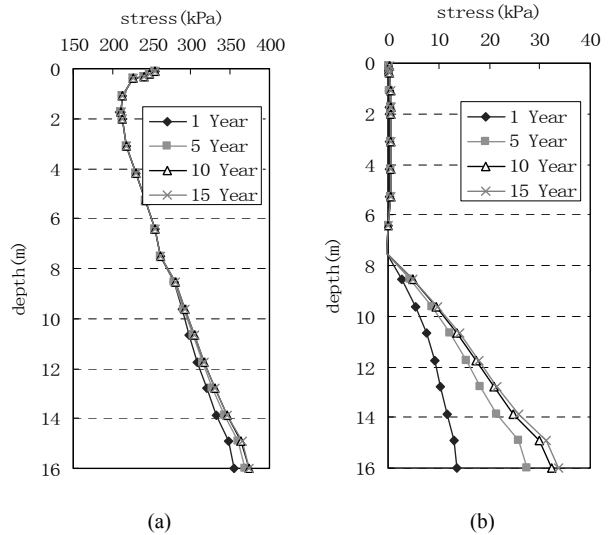


Fig. 14 Increments of vertical effective stress with depth in the soil between the column 1 and column 2: (a) Vertical effective stress and (b) The result of the vertical effective stresses subtracting the stress at T=30day

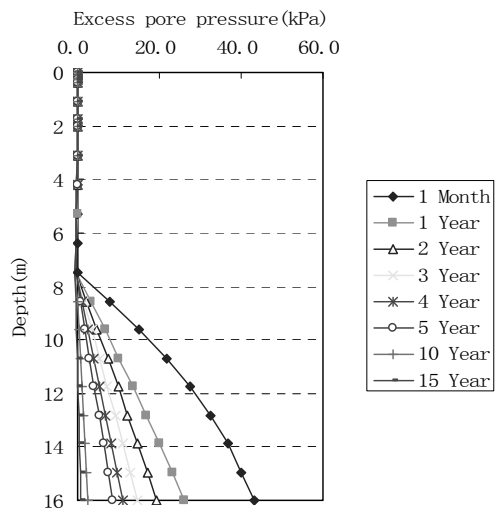


Fig. 15 Excess pore water pressure vs. depth in the soil

PARAMETRIC ANALYSIS OF THE EMBANKMENT

Influence of the deformability of the embankment

The influence of the embankment deformability (E_{emb}) is studied by analyzing two cases with E_{emb} of 5MPa and 20MPa, as illustrated in Fig. 16.

The results in Fig. 16 illustrate that the deformability of the embankment has considerable influence on the magnitude of differential settlements. When the stiffness of the embankment increases, the arching effect developed in the body of the embankment is more intense, so the load transferred to the columns increases, thereby reducing the vertical stresses on the soft soil and consequently the differential settlements.

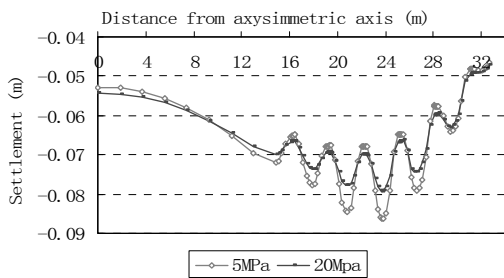
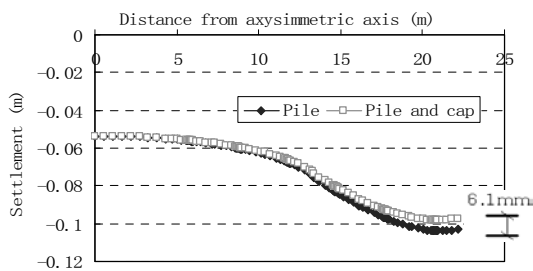


Fig. 16 Influence of the deformability of the embankment on the settlements at the base of the embankment

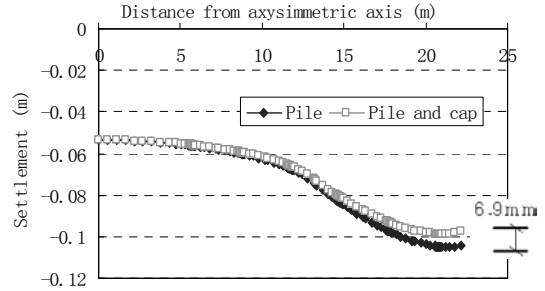
Influence of the effective friction angle of the embankment

The influence of the effective friction angle (ϕ) of the embankment is studied by analyzing two cases with ϕ of 29° , 36° , as illustrated in Fig. 17.

The results in Fig. 17 illustrate that the using of caps has more effect on the settlements when the friction angle of the embankment is smaller. When the effective friction angle is 36° , the reduction of settlement is 6.1mm as caps are used. When the effective friction angle is 29° , the reduction of settlement is 6.9mm. So it can be concluded that the caps can improve the arching effect in the embankment particularly when the friction of the embankment is smaller.



(a) $\phi = 36^\circ$



(b) $\phi = 29^\circ$

Fig. 17 Influence of the effective friction angle of the embankment on the settlements at the crest of the embankment

CONCLUSIONS

The analysis performed in this work illustrated that the coupled mechanical and hydraulic modeling is necessary to study the time-dependant behavior of the column-supported embankment in highway widening project. And the analysis revealed the following aspects:

1. The inclusion of columns causes the decrease of the maximum settlement at the base of the embankment. At the same time, the columns reinforcement induces differential settlements between the soil and the column. These differential settlements increase slightly over time. And the differential settlements of the columns are different. The differential settlement is reduced when the caps are used.

2. The transversal evolution of the vertical displacement has no pattern with depth, whereas close to the surface there is a region ($z > -10.7m$) in which the vertical displacement in the soil is higher than in the columns. In the deep region ($z < -10.7m$) the vertical displacement in the columns is higher than in the soil. The result has a good agreement to Venda Oliveira PJ (2011).

3. Due to the arching effect, the load applied by the embankment is fundamentally concentrated on the columns. When the caps are used, the concentrated stress near the columns is reduced.

4. Increasing the deformability of the embankment originates lower differential settlements, since the relative stiffness of the embankment vs. surrounding soil tends to be higher, inducing an increase in the arching effect. The using of caps has more effect on the settlements when the friction angle of the embankment is smaller, and it can be concluded that the caps can improve the arching effect in the embankment particularly when the friction of the embankment is smaller.

REFERENCES

- Abusharar S. W., Zheng J. J. and Chen B. G. (2009). Finite element modeling of the consolidation behavior of multi-column supported road embankment. *Computers and Geotechnics*, 36(4): 676-685.
- Abusharar S. W. and Han J. (2011). Two-dimensional deep-seated slope stability analysis of embankments over stone column improved soft clay. *Engineering Geology*, 120(4): 103-110.
- Forsman J. and Uotinen V. M. (1999). Synthetic reinforcement in the widening of a road embankment on soft ground. *Twelfth European Conference on Soil Mechanics and Geotechnical Engineering*, Amsterdam, Netherlands: 1489-1496.
- Han J., Huang J., Liu S. Y. and Hong Z. S. (2006). Stresses and deformations induced by widening of existing embankments over soft soils. *Proceedings of the international symposium of lowland technology*, Saga, Japan: 201-205.
- Han J., Sadik O. and Robert L. P. (2007). Numerical analysis of foundation columns to support widening of embankments. *Computers and Geotechnics*, 34(6): 435-448.
- Huang J. and Han J. (2009a). 3D coupled mechanical and hydraulic modeling of a geosynthetic-reinforced deep mixed column-supported embankment. *Geotextiles and Geomembranes*, 27(4): 272-280.
- Huang J., Han J. and Oztoprak S. (2009b). Coupled mechanical and hydraulic modeling of geosynthetic-reinforced column-supported embankments. *J. Geotech. Geoenviron. Eng.*, 135(8): 1011-21.
- Poorooshasb H. B. and Meyerhof G. G. (1997). Analysis of behaviour of stone columns and lime columns. *Computers and Geotechnics*, 20(1): 47-70.
- Terzaghi K. (1943). *Theoretical Soil Mechanics*. New York: John Wiley & Sons.
- Venda O. P. J., João L. P. P. and António A. S. C. (2011). Numerical analysis of an embankment built on soft soil reinforced with deep mixing columns: Parametric study. *Computers and Geotechnics*, 38(4): 566-576.
- Wang H. and Huang X. (2004). Centrifuge model test and numerical analysis of embankment widening on soft ground. *Proceedings of the 8th international conference on applications of advanced technologies in transportation engineering*, Beijing, China: 549-553.
- Zheng J. J., Abusharar S. W. and Wang X. Z. (2008). Three-dimensional nonlinear finite element modeling of composite foundation formed by CFG-lime piles. *Computers and Geotechnics*, 35(4): 637-43.